ALL-FIBER BIDIRECTIONAL OPTICAL PARAMETRIC OSCILLATOR FOR PRECISION SENSING

by

Roopa Gowda

A Thesis Submitted to the Faculty of the

DEPARTMENT OF OPTICAL SCIENCES

In Partial Fulfillment of the Requirements

For the Degree of

MASTER OF SCIENCE

In the Graduate College

THE UNIVERSITY OF ARIZONA

2015

STATEMENT BY AUTHOR

This thesis has been submitted in partial fulfillment of requirements for an advanced degree at the University of Arizona and is deposited in the University Library to be made available to borrowers under rules of the Library.

Brief quotations from this thesis are allowable without special permission, provided that an accurate acknowledgement of the source is made. Requests for permission for extended quotation from or reproduction of this manuscript in whole or in part may be granted by the head of the major department or the Dean of the Graduate College when in his or her judgment the proposed use of the material is in the interests of scholarship. In all other instances, however, permission must be obtained from the author.

SIGNED: Roopa Gowda

APPROVAL BY THESIS DIRECTOR

This thesis has been approved on the date shown below:

Khanh Q. Kieu
Professor of Optical Sciences

08/11/2015
Date

ACHKNOWLEDGEMENT

I would first like to express my sincerely gratitude to my advisor Dr. Khanh Kieu for his continued support and encouragement during my last 3 years as a volunteer and a graduate student. It was a great opportunity and enriching experience for me working under his supervision. Dr. Khanh Kieu was always willing to help me with experiments and share his ideas and suggestions regarding experiments, which tremendously expanded my knowledge in fiber optics, fiber lasers and non-linear optics. After volunteering with him, I got the motivation to pursue a graduate degree in Optics. This dissertation would not have been possible without his persistent help and constructive guidance. I would like to extend my gratitude to Prof. Nasser Peyghambarian who also gave me an opportunity to work in his group and his advices on my projects. I am indebted to Dr. Khanh Kieu and Prof. Nasser Peyghambarian for giving me an opportunity to work in their group and supporting as a graduate student. I would also like to extend my gratitude to Dr. Robert Norwood who advised me on the projects. My deepest appreciation and thanks to Prof. Masud Mansuripur for teaching me E&M, for being supportive and encouraging.

My special thanks to Olga Kropacheva for helping me during my volunteering time. My sincere thanks to Dr. T. N. Nguyen for scientific assistance and interesting discussions. I would like to thank Kyung-jo Kim, Palash Gangopadhyay, and Kaushik Balakrishnan for their availability and suggestions. I would like to acknowledge Pick Chung Lau, Shiva Shahin, Dmitriy Churin, Soha Namnabat, Soroush Mehravar, Yi-Hsin Ou, Joshua Olson, Raj Patil, Robert Baker, and Babak Amirsolaimani. It was a great time and learning experience working with them.

I am also grateful for funding provided by the agencies: Canon USA Inc., Technology Research Initiative Funding (TRIF) from the State of Arizona, and the Roland V. Shack graduate student

endowed scholarship from the College of Optical Sciences. These funding sources allowed me to focus on the interesting research projects during my time at the University of Arizona.

Lastly, I am thankful and indebted to my husband Vishwas and my family for their love, support and guidance all the time.

TABLE OF CONTENT

LIST OF FIGURES

ABSTRACT

The design and performance of an all-fiber, synchronously pumped, bidirectional optical parametric oscillator (OPO) for precision sensing applications is demonstrated. When two counter propagating pulses are overlapped temporarily on the photodetector a narrow beatnote is observed. In our experimental set-up, the generated beatnote has the bandwidth of < 10Hz. OPO gain mechanism provides no interaction between counter propagating beams unlike homogeneous gain medium. All-fiber design removes the need of free space alignment and adjustments. The use of optical fibers helps reduce the required cost, time, and size of the gyroscope. The fiber OPO (FOPO) can potentially provide greater sensitivity for the reason that the frequency shift is directly proportional to the area of the laser cavity and the possibility to lock to a precise optical clock based on optical frequency comb technology. This novel fiber approach would be great for precision measurements including rotation sensing owing to their ultra-large sensing area and sensitivity.

CHAPTER 1

INTRODUCTION

Sagnac effect:

Rotation sensing is an important application in inertial navigation, geodesic monitoring, and fundamental research such as test of fundamental physics [1]. High precision rotation sensors are based on the Sagnac effect which was discovered over a hundred years ago in an effort to prove the existence of the ether [2]. E. Post published a very good review on the Sagnac effect [3].

The "Sagnac effect" was first experimentally demonstrated in 1913 by Georges Sagnac, in a stationary ring interferometer of area 'A' placed on a rotating table. In a rotating inertial frame, two counter propagating light beams see different path lengths hence the difference in roundtrip time between two beams is:

$$\delta t = \frac{4\Omega \,.\, A}{\upsilon^2}$$

Where Ω is the angular rotation rate, υ is the velocity of light in vacuum. The corresponding fringe phase shift in the interference pattern between two beams is:

$$\delta\phi = \frac{8\pi\,\Omega\,.\,A}{\lambda v}$$

Where λ is the wavelength of the beam.

There are two ways of implementing the Sagnac effect, Passive Sagnac interferometers are based on interference between two counter-propagating light fields in a closed loop. The rotation response is detected as a phase shift at the output of the loop. The second implementation provides much better sensitivity and dynamic range and is known as Active Sagnac interferometer. Here, the phase shift will be transformed into the difference in frequency of the laser beams. The closed loop is made into a laser cavity that helps to transform the difference in phase shift experienced by the two counter-propagating optical fields (laser modes) into a frequency shift. So Active Sagnac interferometers are the best device for precision rotation sensing as they provide better sensitivity than the Passive Sagnac interferometers. Using the resonant condition in the laser cavity we can calculate the frequency shift ($\boldsymbol{\delta v}$) and the function of rotation rate ($\boldsymbol{\Omega}$) as follow:

$$L = \mathrm{m}\boldsymbol{\lambda} = \mathrm{m}\frac{\mathrm{c}}{\boldsymbol{v}}$$

$$\boldsymbol{\delta v} = \frac{\boldsymbol{4A}.\Omega}{\lambda L}$$

Where $\boldsymbol{L}$ is the perimeter of the cavity,$\boldsymbol{v}$ is the frequency of the laser field, $\boldsymbol{m}$ is an integer, $\boldsymbol{c}$ is velocity of the light.

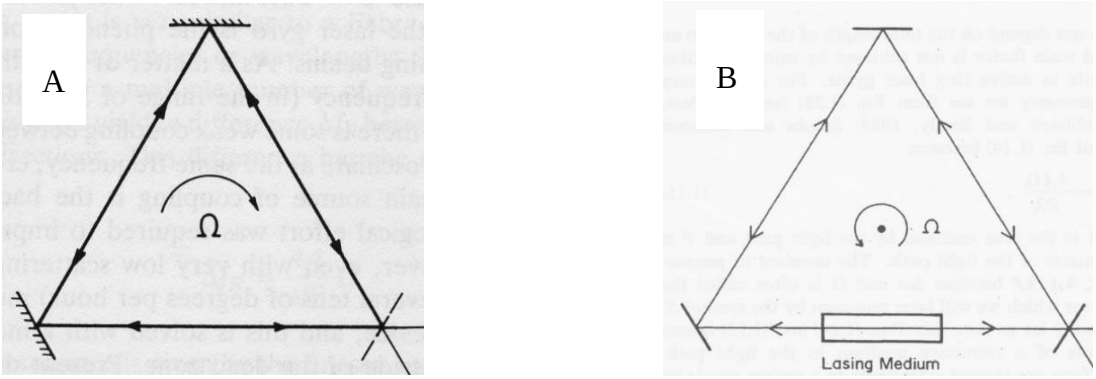

Fig. 1.1. A) Passive Sagnac interferometers are based on the interference between two counter-propagating light fields in a closed loop. The rotation response is detected as a phase shift at the output of the loop. B) Active Sagnac interferometers: the closed loop is made into a laser cavity that helps transform the difference in phase shift experienced by the two counter-propagating optical fields (laser modes) into a frequency shift. (Source of the image: [20])

Lock-in effect:

Beatnote is due to the difference in frequency between the counter propagating beams. At lower rotation rates, the frequencies of counter propagating beams tend to get locked to each other due to coupling between them hence no difference in frequency would be observed. The scatterer injects a part of the light beam from one direction into the opposite direction which couples the light fields. The range of rotation rate over which there is no difference in frequency is called the "Dead-Band". The phase of the scatterer is very crucial in determining the coupling strength hence the shape of the beatnote (Fig. 1.3).

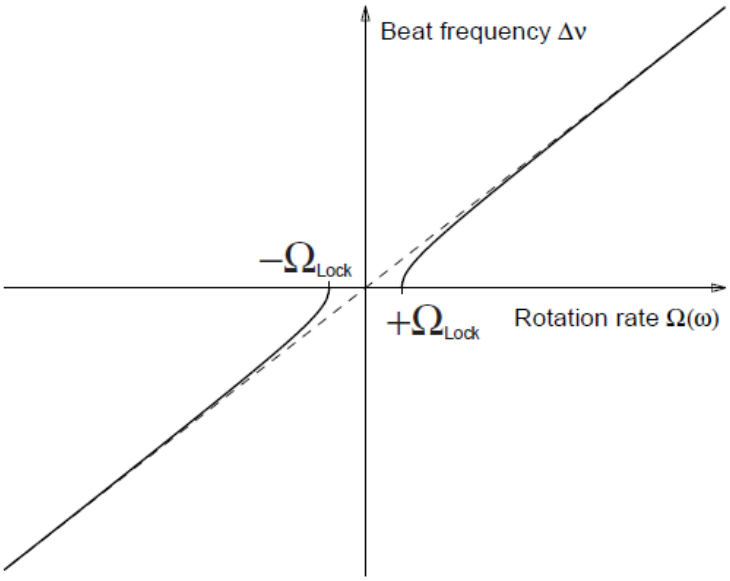

Fig. 1.2. Beat frequency v/s rotation rate. “Dead-Band” is shown for a small range of rotation rates. (Source of the image: [19])

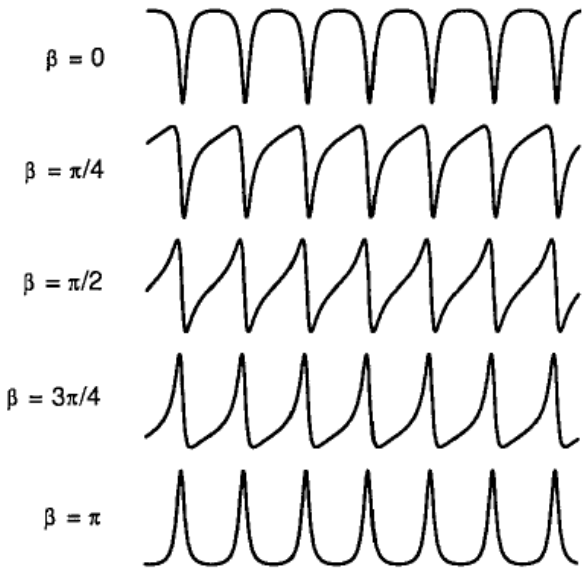

Fig.1.3. Scatterer phase dependant beatnote shape. ***β*** is the phase of the scatterer. (Source of the image: [19])

Bias:

Ideally, the frequency difference between the counter propagating beams is due to rotation. Some external variables like temperature, pressure, EM field, acoustic noise and internal variables like bifringence, Kerr-effect would lead to spurious beatnote called Bias beatnote. This should be mitigated to reduce the beatnote error. So far many methods have been demonstrated to lessen the bias beatnote which will be discussed in the later section.

Dithering:

In the Dead-Band region, by applying artificial bias beat to the laser gyro one can unlock the frequencies. Bias beatnote can be injected by phase modulating the counter propagating beams which will average out the phase error. Mechanical dithering for He-Ne laser gyros, electro-optic phase modulation for pulsed laser gyro are common methods of applying dithering. Harmonic modulation is applying equal, opposite and periodically reversible bias to the counter propagating beams. Random modulation is randomly modulating the phase keeping the average value of the dither to be zero.

Fiber Optical Parametric Oscillator (FOPO):

OPO is an interesting technique to obtain a source of light radiation at wavelengths other than what can be provided via electronic transitions of existing active gain media. OPO is possible in solid state laser gyros by three wave mixing, a non-linear interaction between three waves due to the

second order non-linear induced polarization. Where as in optical fibers the second order non-linearity is zero due to symmetry, so FOPO is possible only by four wave mixing (FWM) due to the third order non-linear induced polarization. OPO is generated only if conservation of energy and momentum takes place. Once phase-matching condition is satisfied, the signal and idler will be generated from noise. One signal and one idler photon is generated by either two photons of the same pump wavelength or different wavelengths in the parametric interaction process. The dispersion profile of the passive fiber, peak power and wavelength of the pump would determine the wavelength of the idler and signal [21]. The dispersion of the gain fiber for FOPO should be close to zero at the pumping wavelength. FOPOs in comparison with solid state OPO are much economical, compact and no alignment is required if an all-fiber design is adopted.

Conservation of energy:

$$\omega_1 + \omega_2 = \omega_3 + \omega_4$$

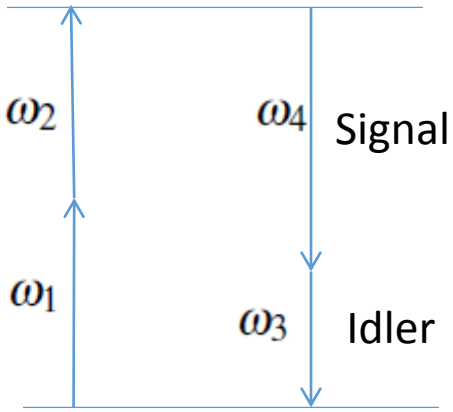

Fig. 1.4. Schematic diagram showing the conservation of energy law

Conservation of momentum:

$$\Delta k_M = \beta_3 + \beta_4 - \beta_1 - \beta_2 = 0$$

$$= (\tilde{n}_3\omega_3 + \tilde{n}_4\omega_4 - \tilde{n}_1\omega_1 - \tilde{n}_2\omega_2)/C$$

Where ω is frequency, ñ mode index, β is propagation constant, k is wave number.

CHAPTER 2

OVERVIEW AND MOTIVATION

He-Ne laser gyros:

The most popular design of an active Sagnac interferometer is based on a ring He-Ne laser which can have a triangular or square shape (the ring laser gyroscope) [4]. These active laser gyroscopes are currently being used in highly demanding applications such as airplanes and satellites navigation. Their level of sensitivity can reach better than part-per-millions of earth rate (which is about 15 degrees an hour). The He-Ne laser gyroscope was developed in the early sixties [5] and they have been almost irreplaceable for precision sensing. It has been also proposed to use them to test fundamental physics like frame dragging, local Lorentz invariance, Time reversal, parity violation theorem and in geophysics for the detection of seismic wave rotation, lunar and solar tides, and fluctuations in the length of the day [1]. The first large ring laser gyroscope of area 0.7547 m^2 named C-1 built at the University of Canterbury. C-1 is the first ring gyro to unlock on earth rotation and could sense the earth rotation rate with a great accuracy of 1 part in 10^{15} of the laser frequency 474 THz [18]. The He-Ne ring laser gyro is a superb instrument, yet some important features are not favorable for all applications. The device is expensive, heavy, bulky, sensitive to electromagnetic interference, and has lifetime limitations. Furthermore, these gyroscopes also suffer from the lock-in effect which results in low sensitivity at small rotation rates [4, 6]. Although mitigation techniques have been developed such as mechanical dithering to unlock the frequencies [4], lock-in is still a major issue in laser-based rotation sensors that can't be dithered.

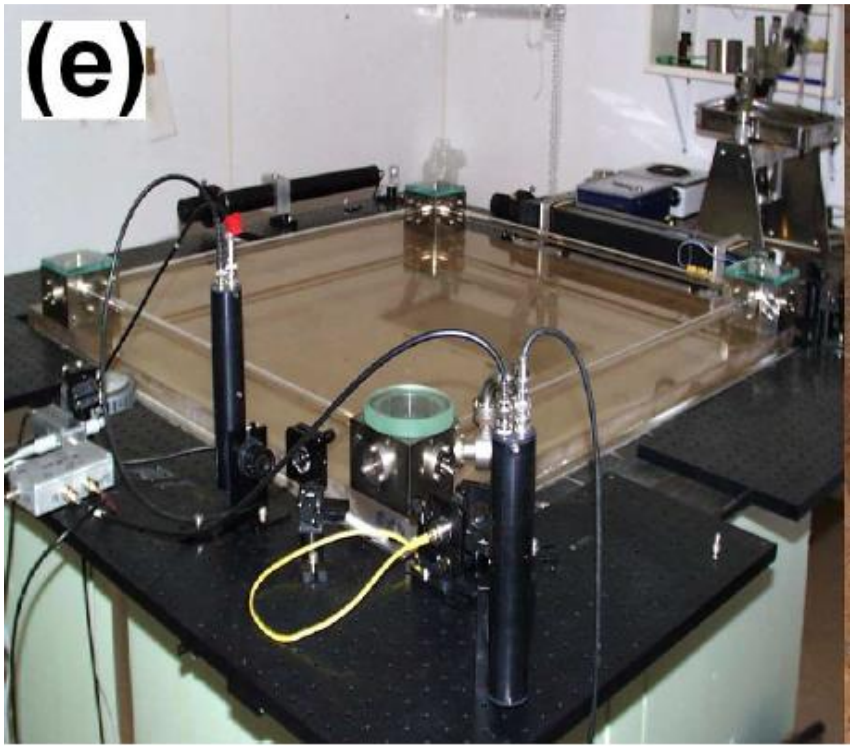

Fig. 2.1. C-1, the first large He-Ne ring laser built at the University of Canterbury which has an area of 0.7547 m^2. (Source of the image: [18])

The frequency shift detected at the output of the gyroscope is proportional to the area covered by the laser cavity. For that reason, it is desirable to have as large of the sensing area as possible to achieve greater sensitivity. Heroic experiments on area scaling have been done in the last two decades by various groups, mainly in Europe [7]. One example is the Gross Ring laser gyroscope located in Wettzell (Bavaria, Germany) which has about $16m^2$ sensing area [7]. The entire ring laser was made out of a monolithic zerodur block to improve mechanical stability. As the result, the device can detect rotation of the earth with ultrahigh level of precision such that it has detected the earth tide, tilt, and the subtle wobbling of the earth's rotation axis over time [8, 9]. The biggest

active laser gyroscope was developed in 2009 which featured an astounding 39.7x21m^2 (or 834m^2) cavity as shown in the fig 2.2. [10].

Fig. 2.2. UG-2 ring laser, the largest He-Ne ring laser built underground at the Cashmere Cavern, Christchurch, New Zealand (latitude of -43.575^0) which has an area of 834m^2. (Source of the image: [18])

However, this is basically the limit of the He-Ne laser technology. The large cavity is not stable enough for long term use due to the massive weight of the support structure where the cavity mirrors are mounted. Gravity pulls the heavy cavity so much that the cavity length is drifting over time and can't be compensated. As the area of the cavity increases, it is harder to control the multimode operation since the separation of the modes decreases also mechanical and thermal

instabilities come in to the picture. The stainless steel used to connect the supermirrors outgases Hydrogen which contaminates the gain medium [18].

In our opinion, there are two important tasks that need to be accomplished: 1) Find a way to increase the sensing area in order to reach higher level of measurement sensitivity; 2) Reduce the required cost, time, complexity, size to build ultrasensitive laser gyroscopes. Clearly, there is a need to develop a new rotation sensing platform if we would like to address the above mentioned challenges.

Fiber optics:

We think fiber optics is a great candidate here. The propagation loss of state-of-the-art optical fibers can be below 0.2dB/km. That means light can propagate through many kilometers of fiber without experiencing significant loss. Optical fibers are also lightweight owing to their small dimension. It is thus possible to construct very large laser cavity (orders of magnitude larger compared to current He-Ne technology) with this platform. It is worth to point out that the large sensing area provided by optical fiber technology is also compatible with compact device size since fiber can be coiled into small loops.

Active fiber laser has been tried as a rotation sensor in the past [11, 12]. However, the level of sensitivity was much worse compared to the He-Ne laser platform. The main reason is that it is quite difficult to achieve single-frequency lasing in both directions of a long cavity fiber laser. The second reason is the same lock-in effect that may be even worse in fiber due to the relatively strong Raleigh scattering which couples to two optical fields. The way out is to use mode-locking instead of CW lasing operation.

Mode-locked laser gyros:

In CW lasers the counter-propagating beams interact with each other all the time due to strict spacial and temporal overlapping. Beams get coupled due to interactions between them (via scattering on imperfections of mirrors) which results in the lock-in effect. This effect can be reduced by minimizing the spatial and temporal overlap of the beams. In mode-locked lasers, locking is significantly reduced since the extension of the ultrashort pulses in space is small compared to the total cavity length [13, 14]. Counter propagating pulses meet only twice in the cavity. By making these two meeting points located at a low scattering medium coupling can be easily reduced. Low scattering medium could be air or vacuum instead at the mirror surfaces. It is possible to build bidirectional mode-locked lasers which generate two ultrashort (in the picosecond or femtosecond time scale) optical pulse trains from the clockwise (CW) and counter-clockwise (CCW) directions of the same cavity. Though short pulses offer an ability to reduce the lock-in effect, nonlinear effects in the cavity can lead to a large bias beatnote. Counter propagating pulses do not see the optical components of the cavity in the same order, so at a given point in the cavity they may have different intensity. Especially, the saturable absorber which is an intensity dependent element can create a non-reciprocal effect because of the difference in intensities [19]. The difference in the intensities can also result in the Kerr non-linear effect. Hence the counter propagating beams may see different refractive indices and will experience different optical path lengths, ultimately causing a bias beatnote.

Other mode-locked lasers gyros:

There are many mode-locked lasers which are discussed below that have been exploited for their practical applications as a gyroscope. Dye lasers gyros provide automatic decoupling between the counter propagating beams due to the motion of the dye molecules in the solution, which has been explained in the literature by three theories, randomizing the phase of the scatterer, Doppler shift and four wave mixing [19]. But they are very messy to handle and noisier due to the short excitation lifetime of laser dyes. Diode lasers are again noisy due to the power supply. They require very fast power supply since they use gain switching mechanism for active mode-locking. The smallest beatnote was measured was at 20kHz and depending on the alignment of the etalons the scale factor would vary from 20kHz to 500kHz [22]. So the alignment controls the scale factor which is not a desirable feature.

Ti:sapphire laser gyro have been demonstrated successfully with different types of saturable absorbers like a dye jet, a piece of Schott glass RG-830, or Kerr-lens effect in the laser cavity [19]. Mode-locked Ti:Sapphire linear cavity gyro has been demonstrated to measure the phase changes in the cavity with a beatnote of 100Hz, the ratio of r(33) to r(13) electro-optic coefficients in $LiNbO_3$ was measured to be 3.57 which is in good agreement with the expected value of 3.62 [23]. The narrowest beatnote from a Ti:sapphire picosecond ring dye laser was about 10Hz [19]. The first Kerr-lens mode-locked femtosecond Ti:sapphire ring laser gyro has been reported to have a beatnote of 70KHz, the beatnote was fluctuating between 20-150kHz depending on the alignment of the laser cavity [24]. As long as the round-trip time is shorter than the excitation lifetime of the mode-locked laser gyros, the longer perimeter of the cavity does not contribute for the sensitivity.

In case of homogeneous gain medium, it is harder to obtain bidirectional lasing due to the gain competition of the counter propagating pulses. This gain competition also results in different amplitude of the pulses.

The first bidirectional mode-locked fiber laser was reported in 2008 where a large biased beatnote was observed at 2MHz with about 2kHz linewidth [15]. This laser is interesting for rotation sensing but requires some further research to establish its full potential. Our unpublished data shows that it is quite difficult to scale the length of the cavity (or the area the cavity encompasses) much further due to complex laser dynamics.

A solution to avoid the interaction of the pulses in the gain medium is optical parametric oscillator (OPO). OPO is a nonlinear effect in which the "excited state lifetime" is same as pump pulse duration time (close to instantaneous interaction).

Prof. Diels group has done extensive research of Bidirectional OPO ring gyros. The first solid-state bidirectional, synchronously pumped, ring optical parametric oscillator was reported in 2001 [16], which was based on a periodically poled lithium nionate crystal and free-space optics which hinders sensing area scaling.

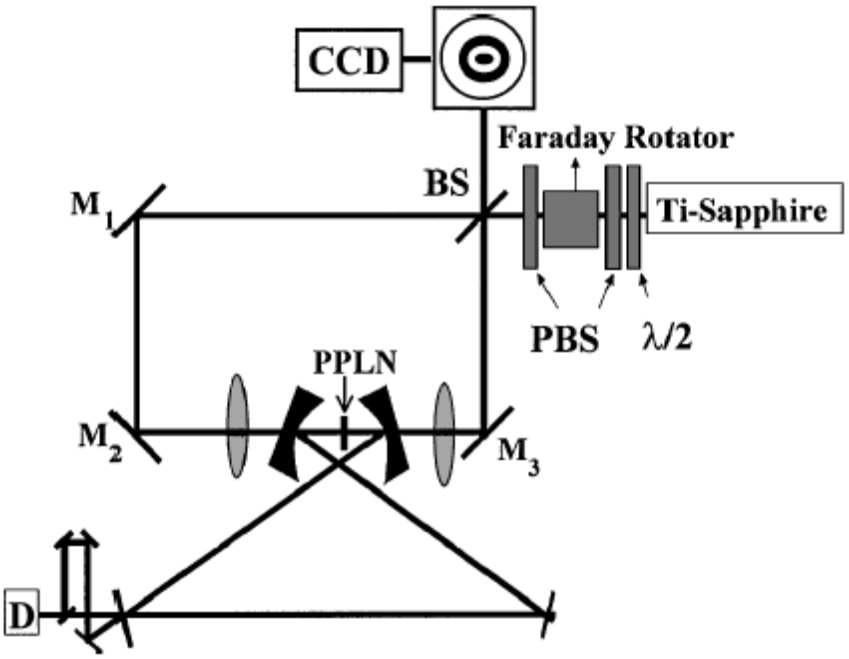

Fig. 2.3. The first solid-state bidirectional, synchronously pumped, ring optical parametric oscillator based on a periodically poled lithium nionate crystal.

Our approach:

In this thesis, we propose a new design of the fiber laser cavity which avoids the complex laser dynamics associated with a gain medium having a relatively long excited state lifetime. We show that it is possible to build a bidirectional mode-locked laser using four-wave-mixing in a suitable optical fiber. This gain mechanism is instantaneous so mode-locking is achieved without many complications. The new design requires a mode-locked fiber laser as a pump source but this is not a difficult requirement anymore since compact, low cost mode-locked fiber lasers have been developed and are currently widely available. Our unique design also provides automatic delay compensation which removes the requirement of having delay line to overlap the output pulses temporally.

CHAPTER 3

EXPERIMENTAL SET-UP

We have tried a couple of different cavity designs for the FOPO, the below mentioned one was the best design since the FOPO cavity is symmetric hence non-reciprocal effects can be minimized. The schematic diagram of the bidirectional FOPO (BiFOPO) is shown in Fig.3.1. We start with a compact Er-doped mode-locked (ML) fiber laser working at 1560nm as the pump source. The laser has a carbon nanotube-based saturable absorber as the mode-locking element [17]. A 980/1550nm

wavelength division multiplexing (WDM) was used to launch the 980nm pump light into the cavity. Er^{3+} doped fiber (EDF) of length <1m was used as a gain fiber. Isolator was to make the cavity unidirectional in an either clockwise or anticlockwise direction. The output was extracted by 80/20 output coupler (OC), 20% out and 80% feedback in to the cavity. Optical delay line is included in the laser cavity to synchronize the laser cavity with the FOPO cavity. The delay line in the laser cavity helps in having the FOPO cavity symmetric so counter propagating pulses see the optical components in the same order. Laser output is made to be linearly polarized by using a polarization controller.

The current laser emits a pulse train at ~35.8MHz design repetition rate and average output power of ~1mW. The output from the ML laser oscillator was amplified to 50mW in a home-built polarization maintaining erbium-doped fiber amplifier (PM EDFA) so that the amplified output from the EDFA was linearly polarized. The length of EDF was about ~1.5m used to amplify the 1560nm signal. Optical spectrum of the pump pulses after the amplifier (at output of ~10mW average power) is shown in the

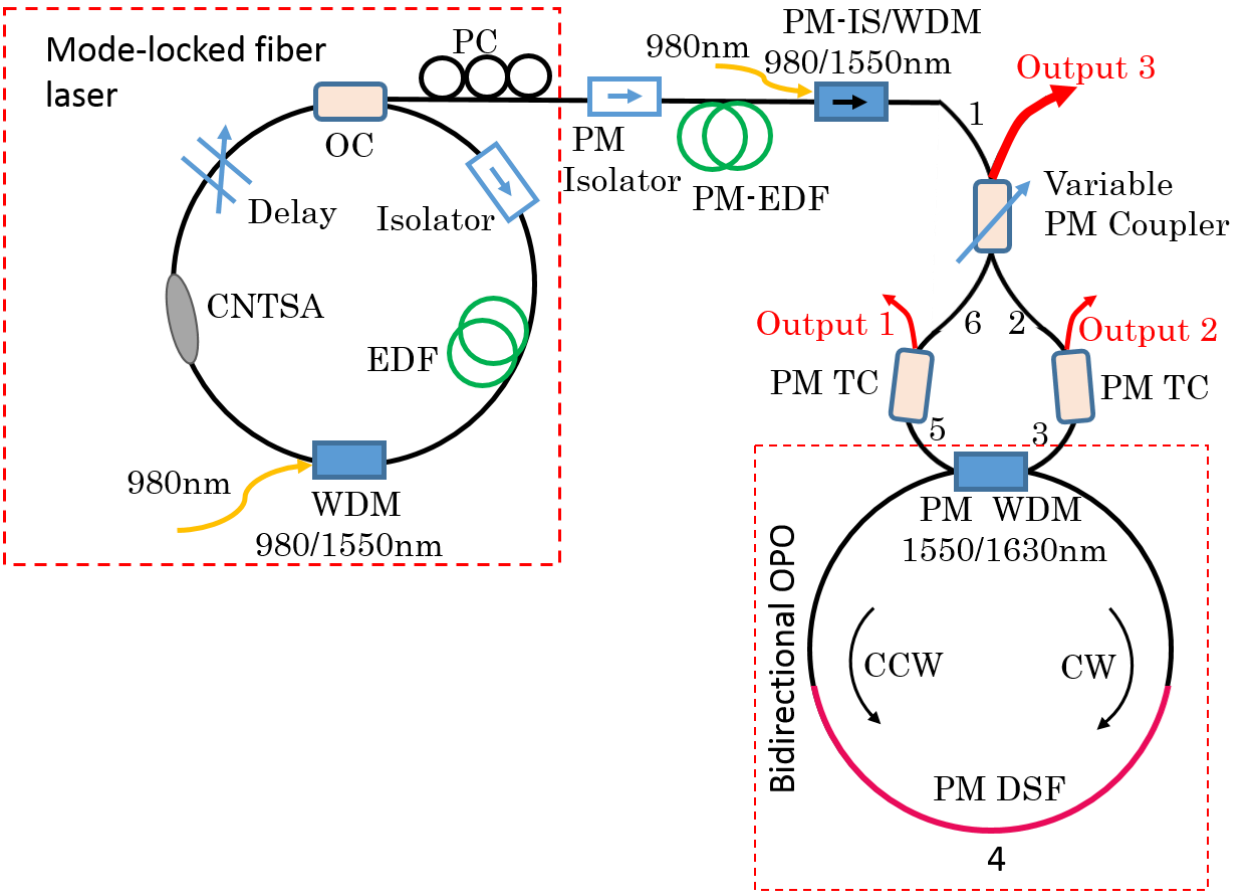

Fig.3.1. Diagram of the bidirectional fiber optical parametric oscillator (FOPO). PC: polarization controller; OC: output coupler; EDF: erbium-doped fiber; WDM: wavelength division multiplexer; CNTSA: carbon nanotubes saturable absorber; TC: tap coupler; PM DSF: polarization maintaining dispersion shifted fiber.

Fig.3.2. The output of the amplifier is split in to two by using a variable PM coupler, the same coupler was used to measure the FOPO output. Fig. 3.3. shows the optical spectrum of pump right after the variable PM coupler measured at the point #6 and #2 with the power ~4.32mW and ~4.48mW, respectively. Two tap output couplers were used to tap out the signal to monitor the FOPO operation from both directions. Fig.3.4. shows the pump laser spectra for the CW (red) and CCW (blue) measured at point #3 and #5, with the power ~4.26mW and ~4.34mW respectively. The BiFOPO cavity is made of a fused PM 2x2 1560/1630nm WDM which also serves as the

output coupler. The parametric gain fiber is a PM dispersion shifted fiber (DSF) manufactured by Corning Inc. The length of the PM DSF is ~5.35m. The rest of the fiber is a standard PM 1550nm fiber with anomalous dispersion of ~ $-23ps^2/km$. Cavity synchronization is achieved by adjusting a delay line which is incorporated into the cavity of the ML Er-doped fiber laser.

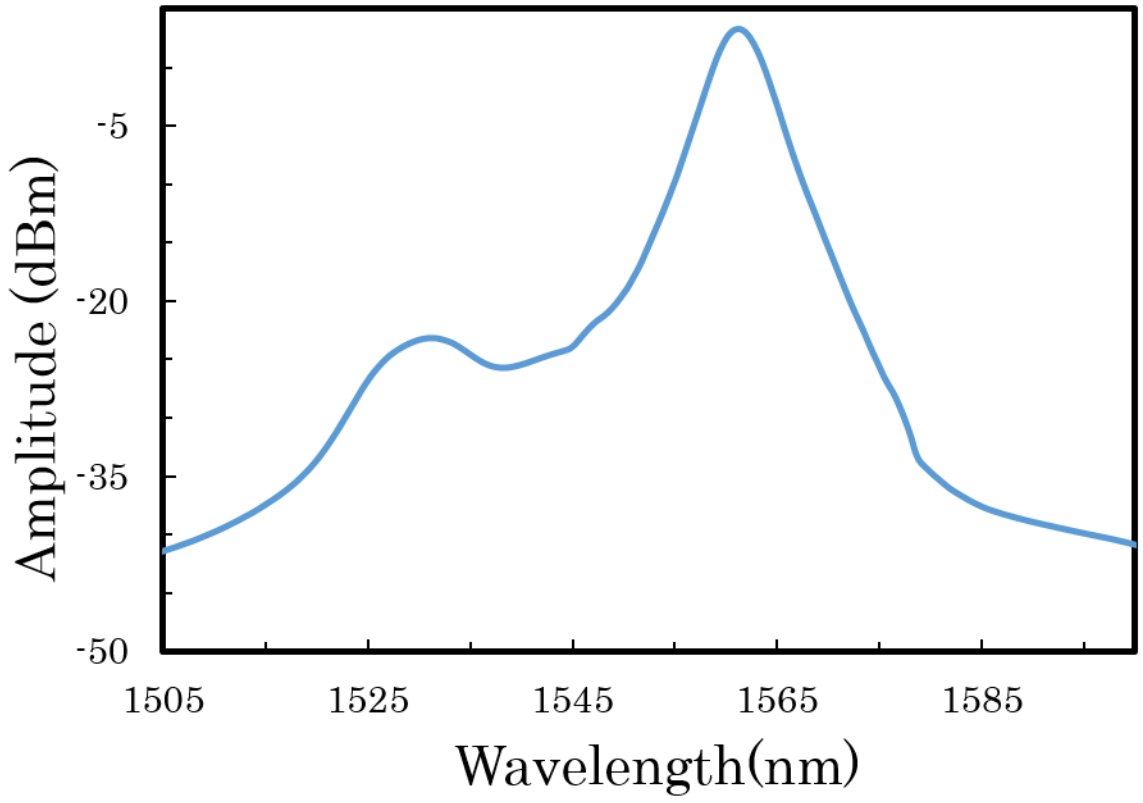

Fig. 3.2. Optical spectrum right after the amplifier measured at the point #1(Fig. 3.1) with the output power ~10mW.

We found that this is a better design since delay lines working in the C-band are commercially available. Two 5% PM tap couplers (TC) are used to monitor the parametric lasing in the CW and CCW direction, respectively. So the 1560nm pulses go through 1-2-3-4-5-6-1 to pump the FOPO in the CCW direction. The sequence is 1-6-5-4-3-2-1 for the CW direction. It turns out that

parametric lasing is achieved quite easily with <5mW pump average power. The pulse pulses have a FWHM spectral bandwidth of~4nm which corresponds to ~800fs transform-limited pulse duration. The pump, signal and idler are co-polarized. The idler signal is the field that is on resonant with the cavity. The repetition rate of the idler pulse trains is identical and is defined by the pump laser repetition rate. Our design resembles a Sagnac loop mirror so the pump pulses meet each other at exactly the same time on the way back after pumping the BiFOPO.

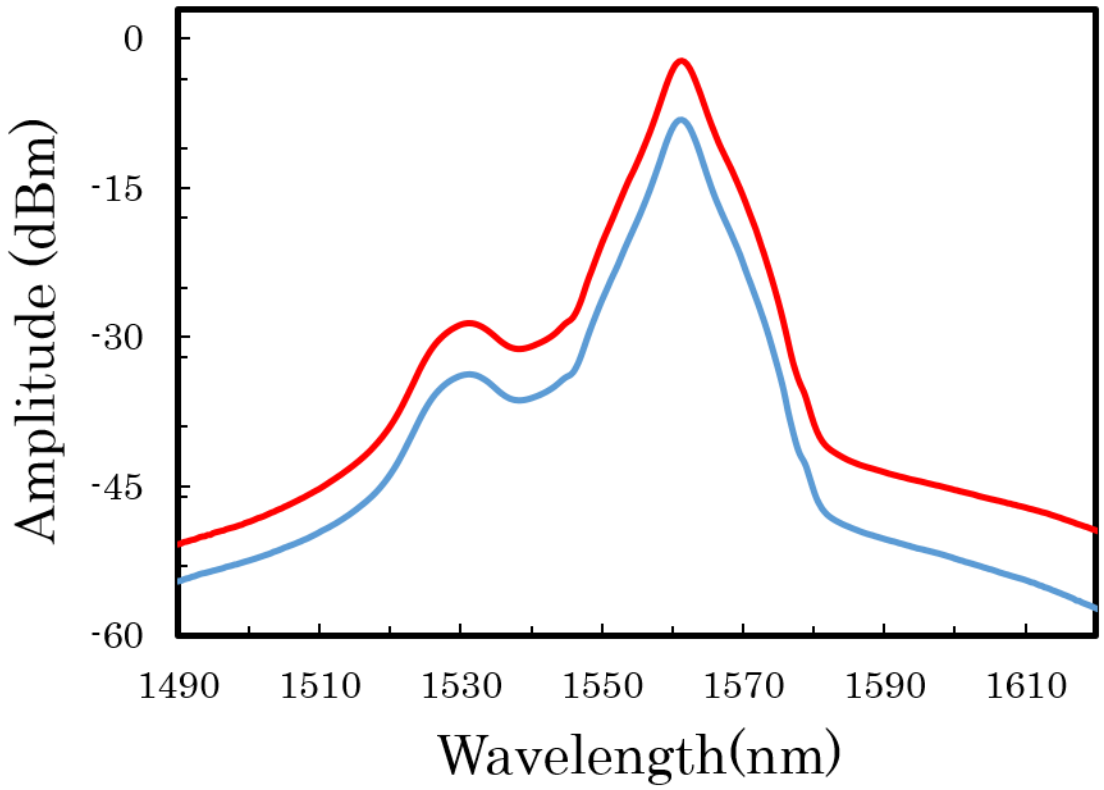

Fig. 3.3. Optical spectrum right after the variable PM coupler measured at the point #6 and #2 with the power ~4.32mW and ~4.48mW, respectively. The red curve is offset by 5dB for better visibility.

As the result the idler pulses generated from each direction must also meet each other at the same time at the point where the pump pulses are split in half (the variable PM coupler). So temporal

overlapping is automatically achieved. This is an important feature which simplifies the beatnote detection step significantly.

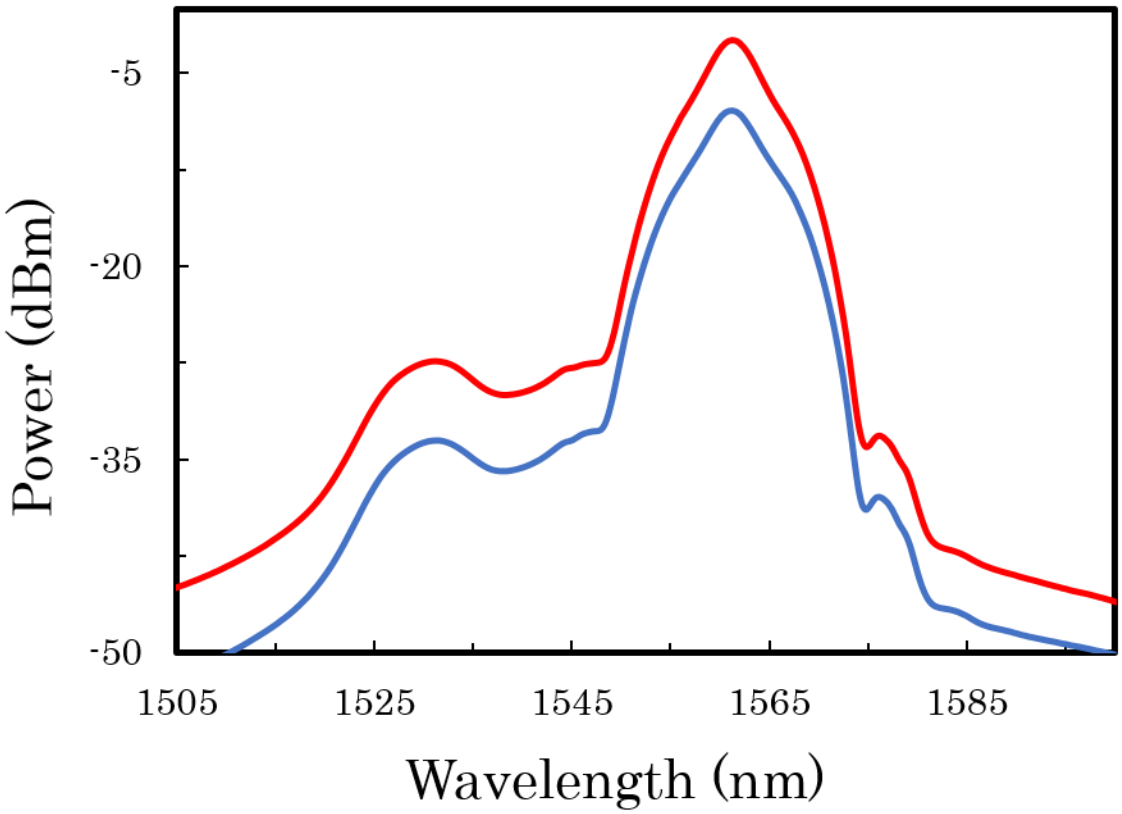

Fig.3.4. The pump laser spectra for the CW (red) and CCW (blue) measured at point #5 and #3, with the power ~4.26mW and ~4.34mW, respectively. The red curve was offset by 5dB for better visibility.

CHAPTER 4

RESULTS AND DISCUSSION

Parametric lasing in both CW and CCW directions are observed as soon as the 1560nm pump power in each direction is increased to >~4mW. Cavity synchronization is ensured by adjusting the delay line in the Er-doped mode-locked seed laser. We calculated the FWM phase matching condition using the dispersion profile of the PM DSF and the pump laser's pulse characteristics. The calculation result is shown in Fig. 3.5. We expect the idler to be at around 1620nm from the graph. Fig. 3.6. shows the output spectra from the BiFOPO measured at various access points (output 1, 2, and 3). The estimated total cavity dispersion of the BiFOPO is ~ -0.014ps^2 which is in the anomalous range. For that reason, our BiFOPO operates in the standard soliton regime at around 1640nm (close to what is expected from the phase matching curve shown in Fib. 3.5.) with Kelly sidebands clearly visible (Fig. 3.6.). The FWHM of the idler spectra (for both CW and CCW directions) is ~8nm corresponding to ~ 400fs transform-limited pulse duration. The operation of the BiOPO is self-starting as soon as the pump is turned on. Bidirectional operation is maintained for weeks without interruption.

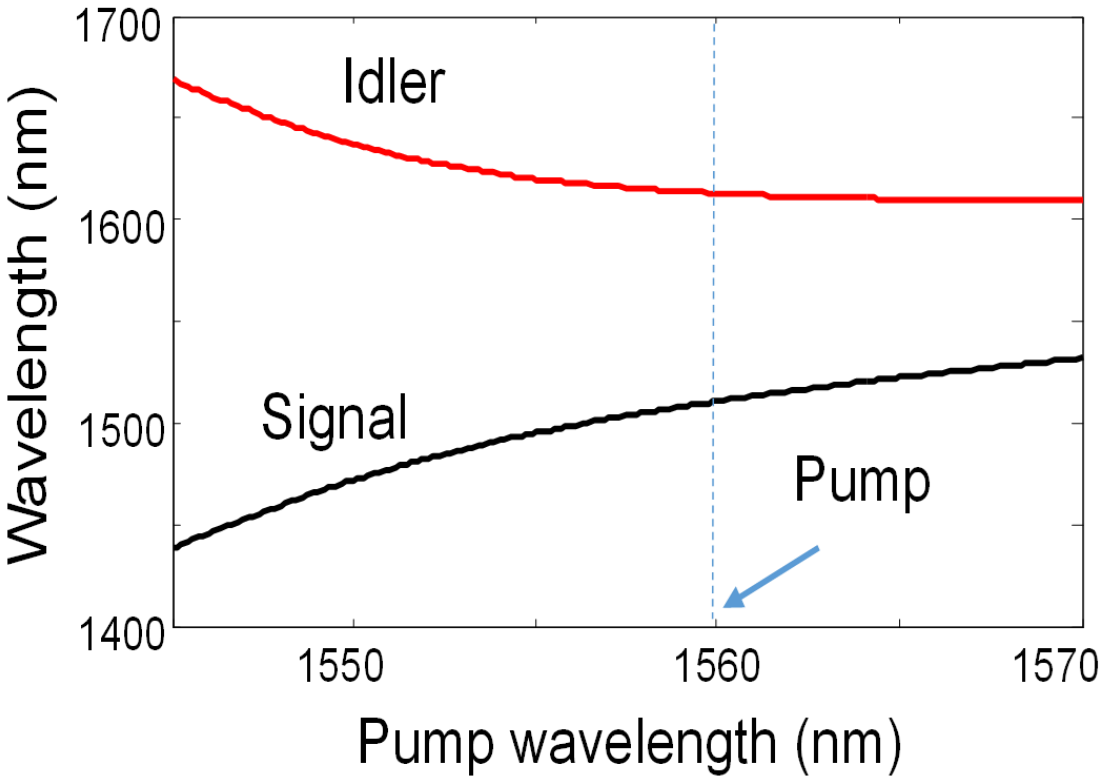

Fig. 4.1. Calculated parametric phase matching curves for the PM DSF. The idler wave is phase-matched at around 1620nm when pumped at 1560nm.

At this point, we have generated two idler pulse trains with identical repetition rate from the CW and CCW directions. In the frequency domain, each pulse train generated in the cavity corresponds to a frequency comb. When the repetition rates of the two pulse trains are equal, the gaps between the neighboring teeth of the combs are identical. However, the carrier frequency offsets of the combs may be different. The reason for this is the difference in the carrier-to-envelop offset (CEO) phase of the pulses. To measure the CEO frequency difference between two laser pulse trains we need to overlap them in time on a photodetector. As mentioned above, the idler pulses from the

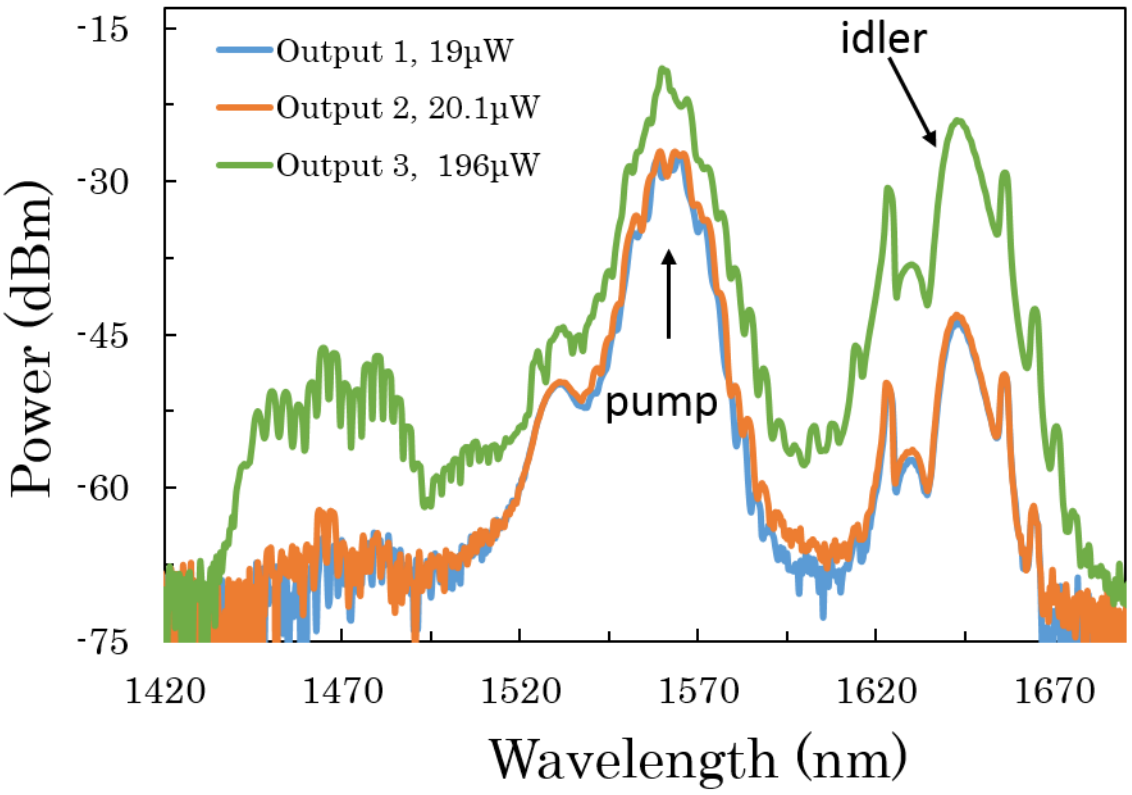

Fig. 4.2. Output optical spectra from the above-threshold BiFOPO. The pump power was ~4.26mW in both directions. The ratio of the idler signal over the pump power is increased at port 3 (compared to port 1 and 2) since most of the pump power is directed back to the PM amplifier (Sagnac loop mirror effect). The idler signals are generated inside the loop so they are split with the ratio of 50/50 at the PM OC.

CW and CCW directions are overlapped in time automatically at the output 3 due to the design of the setup (Sagnac loop mirror effect). The only requirement is that the difference in length of the PM fiber from 2 to 3 and from 5 to 6 must be < ~10cm due to the difference in group velocity for the pump light at 1560nm and the idler (wavelength ~1640nm). There is an induced temporal delay between the pump pulse and the idler pulse as they propagate through the fibers. The estimated temporal delay is ~1.3ps/m for the standard PM fiber. This condition is easily met because the fiber lengths can be matched to <10cm error without significant effort.

Thus, to observe the CEO frequency difference beatnote we just need to put the laser output (from port #3) to a fast photodiode and use an RF spectrum analyzer to visualize the frequency mixing effect. The result of the measurement is shown in Fig. 3.7. We see a strong signal corresponding to the repetition frequency of the laser pulse trains at ~35.8MHz ($f_{rep.}$), as expected. In addition, we observe two strong sidebands symmetrically located on both sides of $f_{rep.}$, which are due to the difference of the CEO frequencies of the two frequency combs.

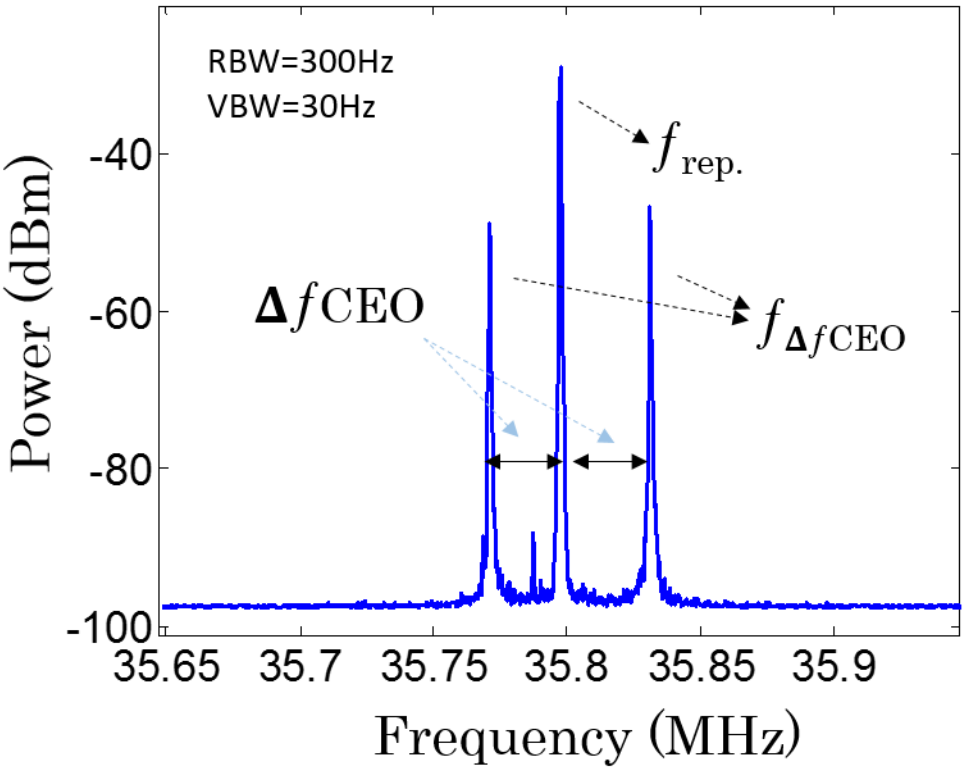

Fig. 4.3. Frequency beating observed when the output from the BiFOPO is detected with a photodiode and the signal analyzed with an RF spectrum analyzer.

The FWHM of the $f_{\Delta ceo}$ beatnotes is ~ 300Hz which is limited by the resolution bandwidth of the RF spectrum analyzer. We observed that the $f_{\Delta ceo}$ beatnotes drift over time due to the environmental noise, temperature change to the laser cavities, or the change of the splitting ratio of the variable PM coupler. This random drift will be a problem that needs to be eliminated when we use the BiFOPO for precision sensing measurements. We can also control the beatnotes by changing the coupling ratio of the PM variable coupler. This effect is explained by the power misbalance leading to an appreciable non-reciprocal nonlinear phase shift which can affect the CEO frequency difference.

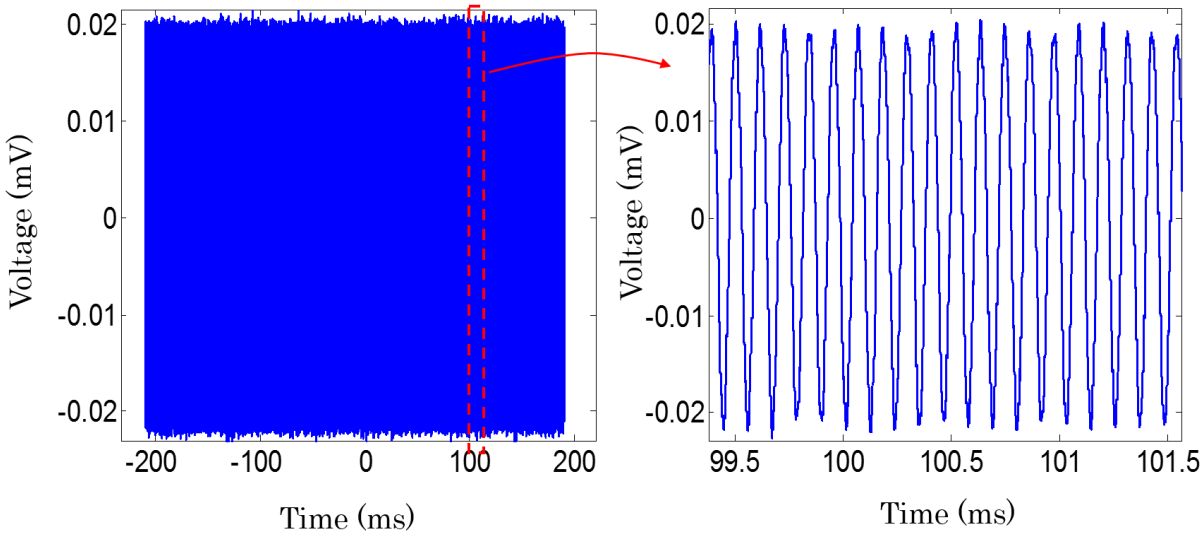

Fig. 4.4. Time-domain signal resulted from the beating of the two frequency combs (generated from the BiFOPO) on a slow photodiode. The measurement span is ~400ms which corresponds to about 2.5Hz resolution in the frequency domain. The sampling rate was 5MS/s.

The FWHM linewidth of the $f_{\Delta ceo}$ beatnotes will eventually define the sensitivity of the device for rotation sensing application (or other applications such as magnetic field measurement). To accurately estimate the linewidth of the $f_{\Delta ceo}$ we use time-domain measurements. We record the voltage from a slow photodiode (~2MHz bandwidth, to filter out the high frequency

components) using an AC coupled digital oscilloscope. We observe a clean sinusoidal signal on the oscilloscope screen (Fig. 3.8.). The time-domain signal is Fourier-transformed to find the corresponding frequency. The resolution in the frequency domain is defined by the measurement span in time. From the data shown in Fig. 3.9. We estimate the FWHM of the $f_{\Delta ceo}$ beatnote is in the order of ~5Hz.

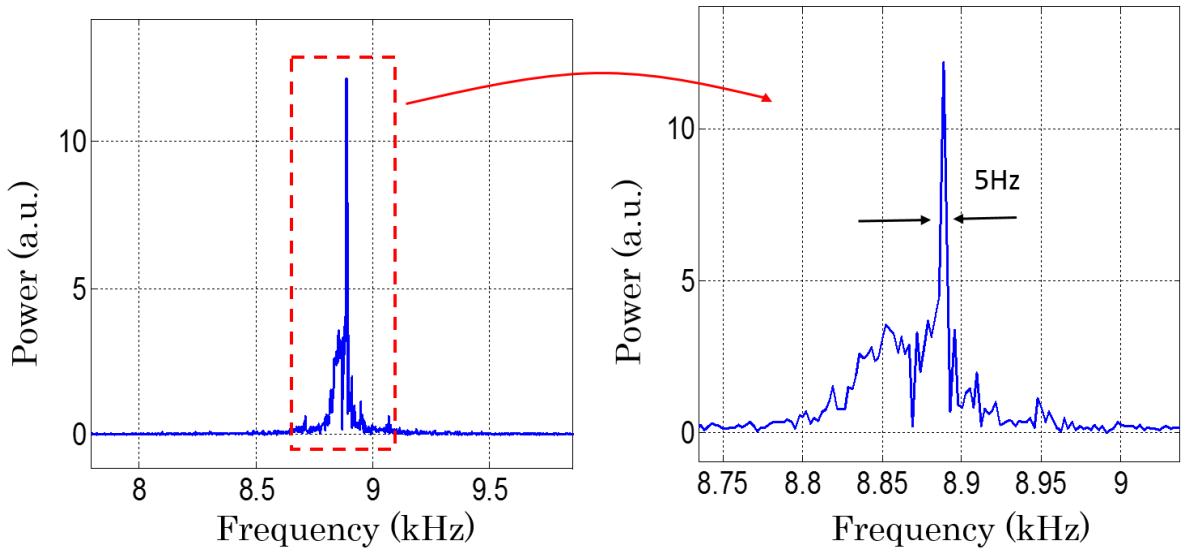

Fig. 4.5. Fourier transform of the time domain signal reveals a narrow peak at around 8.9 kHz with ~5Hz FWHM linewidth.

The center frequency of the beatnote drifts over time so it was difficult to have a longer time span to accurately measure the linewidth of the $f_{\Delta ceo}$. To quantify the drift of the $f_{\Delta ceo}$ beatnote over time, we measure the center frequency of the beatnote with a frequency counter. A typical result of the measurements is shown in Fig. 3.10. The drift is quite significant, which is about tens of kHz over 30 seconds. This will be the main issue that we will have to address in the future to make the technique really useful for precision measurements. It is worth to mention that our setup is not currently isolated from vibrations, temperature

fluctuations. The diode pump laser is not stabilized as well as the erbium-doped mode-locked fiber laser. We think the drift may be significantly reduced by packaging the whole system better to eliminate environmental noise. It will be also interesting to use a fully stabilized Er-doped frequency comb as the pump source to avoid the noise transferred from the pump laser to the BiFOPO. The splitting ratio of the PM variable coupler will also need to be stabilized to ensure stable pump laser power in each direction.

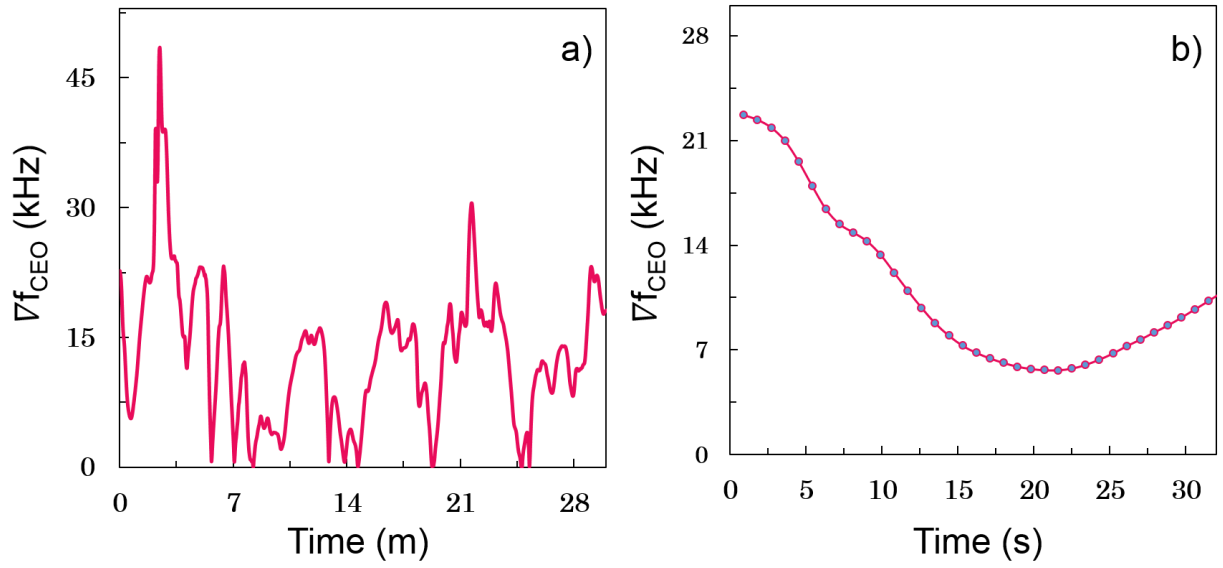

Fig. 4.6. Drift of the difference in the CEO frequencies (Δf_{ceo}) of the two combs generated from the BiFOPO as a function of time.

Fundamental limit to the beatnote is ultimately the shot-noise limited beatnote which is due to the quantum nature of photons. In order to obtain the shot-noise limited beatnote the set-up should be free from the external and internal fluctuations. Shot-noise varies as a square root of the power [20]. As mentioned above the power loss in the fiber increases with length of the fiber 0.2dB/km and the sensitivity of the Sagnac interferometer increases with the length of the fiber. So for a given sensitivity the fiber length is set by the power loss and Sagnac effect. To have sensitivity of

10^{-3} deg/h the length should be approximately few km [20] (I don't really understanding your reasoning here. Maybe we should discuss this point?).

Many methods have been tried in the literature to suppress the bias beatnote. Modulating the intensity of the source to adjust the nonlinear interaction between the counterproapgating waves to reduce the Kerr effect in fiber-optic gyroscopes has been demonstrated experimentally [43]. By reducing the number of splices in the cavity, the power differences can be controlled. The common method to subtract the source intensity noise is to measure the noise at the far end of the source coupler and then electronically subtracting it from the gyro output. In this method, it is difficult to servo the output of the source at high frequencies, so all-optical intensity-noise subtraction scheme has been discussed [44]. Different phase-modulation has been studied to reduce the bias ([45], [46]). Even though the line integral of the magnetic field along the fiber vanishes, the environmental magnetic fields causes the bias beatnote. Earth's magnetic field creates a bias beatnote of 10^{0}/h and it can be reduced by 1 order of magnitude by shielding the fiber coil [47]. Polarization of the fiber should be maintained to avoid bifringence dependent bias beatnote, using PM fibers, polarization holding fibers, polarization scrambling are the few methods that have been reported ([48], [49]). Rayleigh backscattering noise in the fiber-optic gyroscope has been calculated and it was shown that Rayleigh backscattering noise can be minimized by having power-splitting ratio of the fiber loop K = 0.5 [50]. The coherence of the Rayleigh backscattering with the primary waves is determined by the temporal coherence of the source, so it's desirable to have low coherence sources ([51], [52], [53]).

CHAPTER 5

CONCLUSION

In summary, we have demonstrated an all-fiber, synchronously pumped, bidirectional optical parametric oscillator. The laser generates two highly coherent frequency combs with identical repetition rates but slightly different CEO frequencies. The linewidth of the beatnote between the two frequency combs is very narrow in the order of <10Hz indicating the great potential of the setup for precision measurements. The main advantage of the BiFOPO is the possibility to scale up the sensing areas by orders of magnitude compared to the He-Ne laser gyroscope technology. We would like to point out that the area of the BiFOPO can be scaled up without the need to change the repetition rate (or the cavity length) of the pump laser since we can have *N* pump pulses in the OPO cavity at a time, where *N* is a non-zero integer. The remaining challenge is the fact that the center frequency of the beatnote drifts over time. So far, many experiments to find the source of the bias beatnote have been demonstrated, we have discussed some of them. Many novel methods have been exploited to eliminate or minimize the bias beatnote. By implementing those methods we should be able to isolate the system from the fluctuations hence minimize the error. We hope that our BiFOPO has a great ability to provide the greatest sensitivity and reliability that has not been seen before, taking the precision sensing technology ahead. Future work will need to be carried out to get the better understanding of the sources of the drift in order to eliminate them.

REFERENCE:

[1] G. E. Stedman, “Ring laser tests of fundamental physics and geophysics,” Rep. Prog. Phys. 60, 615–688 (1997)

[2] G. Sagnac, "L'éther lumineux démontré par l'effet du vent relatif d'éther dans un interféromètre en rotation uniforme, *Comptes Rendus* **157**: 708– 710 (1913)

[3] E. J. Post, “Sagnac effect,” Rev. Mod. Phys. 39, 475 (1967).

[4] W. W. Chow, J. Gea-Banacloche, L. M. Pedrotti, V. E. Sanders, W. Schleich, and M. O. Scully, “The ring laser gyro,” Rev. Mod. Phys. **57**, 61 (1985).

[5] Warren M. Macek and D. T. M. Davis, Jr. "Rotation rate sensing with traveling-wave ring lasers," *Applied Physics Letters*, vol. **2**, pages 67–68. (1963)

[6] L. M. Menegozzi, W. E. Lamb, “Theory of a ring laser,” Phys. Rev. A **8**, 2103 (1973).

[7] Schreiber, Karl Ulrich and Wells, Jon-Paul R., “Invited Review Article: Large ring lasers for rotation sensing,” Review of Scientific Instruments, **84**, 041101 (2013), DOI:http://dx.doi.org/10.1063/1.4798216

[8] K. U. Schreiber, G. E. Stedman, and T. Klügel, “Earth tide and tilt detection by a ring laser gyroscope,” J. Geophys. Res. **108** (B2), 2132, doi:10.1029/2001JB000569 (2003).

[9] K. U. Schreiber, T. Klügel, J.-P. R. Wells, R. B. Hurst, and A. Gebauer, “How to detect the Chandler and the annual wobble of the earth with a large ring laser gyroscope,” Phys. Rev. Lett. **107**, 173904 (2011)

[10] R. B. Hurst, G. E. Stedman, K. U. Schreiber, R. J. Thirkettle, R. D. Graham, N. Rabeendran, and J.-P. R. Wells, “Experiments with an 834 m2 ring laser interferometer,” J. Appl. Phys. **105**, 113115 (2009)

[11] F. Zarinetchi, S. P. Smith, and S. Ezekiel, "Stimulated Brillouin fiber-optic laser gyroscope," Opt. Lett. **16**, 229-231 (1991)

[12] S. K. Kim, H. K. Kim, and B. Y. Kim, "Er^{3+}-doped fiber ring laser for gyroscope applications," Opt. Lett. **19**, 1810-1812 (1994)

[13] D. Gnass, N.P. Ernsting, and F.P. Schafer, “Sagnac effect in the colliding-pulse-mode-locked dye ring laser” Appl. Phys. B **53**, 119 (1991).

[14] M.L. Dennis, J.-C.M. Diels, and M. Lai, “Femtosecond ring dye laser: a potential new laser gyro,” Opt. Lett. **16**, 529 (1991).

[15] K. Kieu and M. Mansuripur, "All-fiber bidirectional passively mode-locked ring laser," Opt. Lett. **33**, 64-66 (2008)

[16] Xianmei Meng, Jean-Claude Diels, Dietrich Kuehlke, Robert Batchko, and Robert Byer, "Bidirectional, synchronously pumped, ring optical parametric oscillator," Opt. Lett. **26**, 265-267 (2001)

[17] K. Kieu and M. Mansuripur, "Femtosecond laser pulse generation with a fiber taper embedded in carbon nanotube/polymer composite," Opt. Lett. **32**, 2242-2244 (2007).

[18] Nishanthan Rabeendran , “ A study of Ring Laser Gyroscopes” Master Thesis, University of Canterbury, 2008.

[19] Matthew J. Bohn, “The Ti:Sapphire Ring Laser Gyroscope” Ph.D. Thesis, University of New Mexico, 1998.

[20] budker.berkeley.edu/Physics208/Laser%20Gyroscope.ppt

[21] Dmitriy Churin, “Development of ultrafast fiber laser sources” Ph.D. Thesis, university of Arizona, 2015.

[22] W.R. Christian and M.J. Rosker,” Picosecond pulsed diode ring-laser gyroscope” Optics Letters, 16(20):1587-1589, October 1991.

[23] M.J. Bohn and J.-C. Diels, “Measuring intracavity phase changes by use of double pulses in a linear cavity”. Optics Letters,22(9):642-644,May.

[24] M.J. Bohn and J.-C. Diels. Bidirectional Kerr-lens mode-locked femtosecond ring laser. Optics Communications, 141:53-58, August 1997.

[25] M. Lai, J.-C. Diels, and M. L. Dennis, “Nonresiprocal measurements in femtosecond ring lasers. Opt.Lett. 17:1535-1537, 1992.

[26] Briggs Atherton, Scott Diddams, and J.-C. Diels, “Ultrasensitive phase measurements with femtosecond ring lasers”. IN F. W. Wise and C. P. J. Barty, editors, Proceedings of SPIE in Generation. Amplification, and Measurement of Ultrashort Laser Pulses *II*, Vol. 2377, Bellingham, WA, 1995.

[27] W. Macek and D. T. Davis Jr. “Rotation rate sensing with travelling-wave ring lasers. Appl. Phys. Lett., 2:67-68, 1963.

[28] J. M. Dudley, D. T. Reid, M. Ebrahimzadeh, and W. Sibbett, “Characteristics of a non-critically phase matched Ti:sapphire pumped femtosecond optical parametric oscillator” Optics Communications, 104(4,5,6):419-430,January 1994.

[29] D. S. Butterworth, S. Girard, and D. C. Hanna, “A simple technique to achieve active cavity-length stabilization in a synchronously pumped optical parametric oscillator” Optics Commutations, 123:577-582, February 1996.

[30] A. Hache, G.R. Allan, and H.M. van Driel, “Effects of cavity detuning on the pulse characteristics of a femtosecond synchronously pumped optical parametric oscillator” J.Opt. Soc. Am. B, 12(11):2209-2213, November 1995.

[31] T. Kartloglu, K.G. Koprulu, and O. Aytur, “phase-matched self-doubling optical parametric oscillator” optics Letters, 22(6):280-282, March 1997.

[32] P. E. Powers, C. L. Tang, and L.K. Cheng, “High-repetition-rate femtosecond optical parametric oscillator based on CsTiOAso4. Optics letters, 19(1):37-39, January 1994.

[33] D. T. Reid, M. Ebrahimzahed, and W. Sibbett, “Noncritically phase-matched Ti:Sapphire-pumped femtosecond optical parametric oscillator based on RbTiOAsO4. Optics Letters, 20(1):55-57, January 1995.

[34] J. D. Kafka, M L. Watts, and J. W. Pieterse, “Synchronously pumped optical parametric oscillators with LiB3O5” J. Opt. Soc. Am. B, 12(11):2147-2157, November 1995.

[35] M. Ebrahimdeh, S. French, and A. Miller, “Design and performance of a singly resonant picosecond LiB3O5 optical parametric oscillator synchronously pumped by Ti:sapphire laser” J. Opt. Soc. Am. B, 12(1):2180-2191, November 1995.

[36] D. E. Spence, S. Wielandy, C. L. Tang, C. Bosshard, and P. Gunter, “High-repetition-rate femtosecond optical parametric oscillator based on KNbO3” Optics Letters, 22(9):618-682, April 1995.

[37] S. D. Butterworth, P. G. R. Smith, and D. C. Hanna, “Piosecond Ti:sapphire-pumped optical parametric oscillator based on periodically poled LiNbO3” , Optics Letters, 22(9):618, May 1997.

[38] K. Schneider, P. Kramper, S. schiller, and J.Mlynek, “Toward an optical synthesizer: A single-frequency parametric oscillator using periodically poled LiNbO3” Optics Letters, 22(17):1293, September 1997.

[39] W. S. Pelouch, P. E. powers and C. L. Tang, “Ti:sapphire-pumped, high-repetition-rate femtosecond optical parametric oscillator”. Optics Letters, 17(15):1070-1072, August 1992.

[40] C. Fallenich, B. Ruffing, Th. Hermann, A. Nebel, R. Beigang, and R. Wallestein. “Experimental investigation and numerical simulation of the influence of resonator-length detuning on the output power, pulse duration and spectral width of a cw mode-locked picosecond optical parametric oscillator”. Appl. Phys. B, 60:427-436, 1995.

[41] J. E. Rothenberg. “Observation of the transient expansion of heated surfaces by picosecond photothermal deflection spectroscopy”. Optics Letters, 13(9):713-716, September 1988.

[42] G. P. Agrawal, Non-linear Fiber Optics, Academic Press, Boston, MA, 2007.

[43] R. A. Bergh, H. C. Lefevre, and H. J. Shaw, “Compensation of the optical Kerr effect in fiber-optic gyroscopes”. Optics Letters, Vol.7, No. 6, (1982).

[44] Pavel Polvnkin, Josiel de Arruda, and James Blake, “All-optial noise-subtraction scheme for a fiber-optic gyroscope”. Optics Letters, Vol.25, No. 3 (2000).

[45] B. Y. Kim and J. Shaw, “ Gated phase-modulation approach to fiber-optic gyroscope with linearized scale factor”, Optics Letters, Vol.9, No. 8, 1984.

[46] A. Ebberg and G. Schiffner, “ Closed-loop fiber-optic gyroscope with a sawtooth phase-modulation feedback”. Optics Letters, Vol. 10, No. 6 (1985).

[47] K. Bohm, K. Petermann and E. Weidel, “Sensitivity of a fiber-optic gyroscope to environmental magnetic fields”. Optics Letters, Vol. 7, No. 4, (1982).

[48] W. K. Burns, R. P. Moeller, C. A. Villarruel and M. Abebe, “fiber-optic gyroscope with polarization-holding fiber”. Optics Letters, Vol. 8, No. 10 (1983).

[49] Pie-Yau Chien and Ci-Ling Pan, “Fiber-optic gyroscopes based on polarization scrambling”. Optics Letters, Vol. 16, No.3 (1991).

[50] Kazumasa Takada, “Calculation of Rayleigh backscattering noise in fiber-optic gyroscopes”. J. Opt. Soc. Am. A, Vol. 2, No. 6, (1985).

[51] C. C. Cutler, S. A. Newton, and H. J. Shaw, “Limitation of rotation sensing by scattering”. Opt. Lett.5, 488 (1980).

[52] K. Bohm, P. Marten, K. Petermann, E. Weidel and R. Ulrich, “Low-drift fiber gyro using a super luminescent diode”, Electr. Lett. 17, 352 (1981).

[53] K. Bohm, P. Russer, E. Weidel, and R. Ulrich, “Low-noise fiber-optc rotation sensing”, Opt. Lett. 6, 64 (1981).

[54] K. A. Fesler, M. J. F. Digonnet, B. Y. Kim, and H. J. Shaw, “Stable fiber-sourcegyroscopes”, Opt. Lett. 15, 22 (1990).

[55] Clive H. Rowe, Ulrich K. Schreiber, Steven J. Cooper, B. Tom king, Morrie Poulton, and Geoffrey E. Stedman, “Design and operation of a very large ring laser gyroscope”, Applied Optics, Vol. 38, No. 12, (1999).

[56] K. Petermann, “Intensity-dependent nonreciprocal phase shift in fiber-optic gyroscopes for light sources with low coherence”, Opt, Lett. Vol. 7, No. 12 (1982).

[57] R. A. Bergh, H. C. Lefevre, and H. J. Shaw, “All-single-mode optic gyroscope with long-term stability”, Opt. Lett. Vol. 6, No. 10 (1981).

[58] K. U. Schreiber, A. Gebauer and J.-P. R. Wells, “Long-term frequency stabilization of a 16m^2 ring laser gyroscopes”. Opt.Lett. Vol. 37, No. 11 (2012).